Exposing the human *nude* phenotype

The recent discovery of the human counterpart of the *hairless* mouse phenotype[1] has helped our understanding of the molecular genetics of hair growth. But there are no reports of a defect in the human homologue of the best known of the 'bald' mouse phenotypes, the *nude* mouse[2]. This may be because affected individuals are so gravely ill from the accompanying immunodeficiency that their baldness goes unnoticed. We have carried out a genetic analysis that reveals a human homologue of the *nude* mouse.

The *nude* mouse is characterized by a congenital absence of hair and a severe immunodeficiency[2], resulting from mutations in the *whn* (*winged-helix–nude*; *Hfh11*^{nu}) gene, which encodes a member of the forkhead/winged-helix transcription factor family with restricted expression in thymus and skin[3]. The simultaneous occurrence of severe functional T-cell immunodeficiency, congenital alopecia and nail dystrophy (MIM database no. 601705) in two affected sisters led to the recognition that the clinical phenotype was reminiscent of the *nude* mouse[4]. We therefore investigated whether this syndrome represents the human counterpart of the *nude* mouse phenotype.

We obtained DNA samples from members of the sisters' family in a small village in southern Italy. The affected sisters were born with a complete absence of scalp hair (Fig. 1a), eyebrows and eyelashes and had dystrophic nails, and no thymic shadow was evident upon X-ray examination. The first affected child revealed a striking impairment of T-cell function shortly after birth, and died at the age of 12 months. Her sister had similar immunological abnormalities, but bone-marrow transplantation at five months of age led to full immunological reconstitution, although the alopecia and nail dystrophy are still present[4].

We performed linkage analysis using microsatellite markers near the human *WHN* locus on chromosome 17, and found a lod score of 1.32, suggestive of linkage. We then sequenced the human *WHN* gene[5] and found a homozygous C-to-T transition at nucleotide position 792 of the *WHN* cDNA (GenBank accession no. Y11739) (Fig. 1b). This leads to a nonsense mutation at residue 255 (R255X) in exon 5, and predicts the complete absence of functional protein as a result of nonsense-mediated decay of messenger RNA.

Because the proband's bone-marrow transplant was from her brother, we examined her leukocyte DNA both before and after the graft for the presence of chimaerism. Genotyping the proband before the transplant showed that her leukocyte DNA was homozygous only for the mutant allele (Fig. 1c). Four years after the transplant, we detected the haplotype specific for the wild-type paternal *WHN* allele received from the brother, as well as the mutant allele, indicative of chimaerism. Gender determination revealed that the proband's leukocyte DNA was genotypically XX before the transplant, and the brother's DNA was XY. Afterwards, the proband's leukocyte DNA was found to be XY (Fig. 1c), providing evidence of long-term engraftment and expansion of the bone-marrow graft.

The *WHN* gene encodes a transcription factor, which is developmentally regulated and directs cell-fate decisions[6]. In mammals, *whn* is expressed specifically in the epithelial cells of the skin and thymus, where it helps to maintain the balance between growth and differentiation[7,8]. Recent evidence[9] has highlighted the importance of the thymic microenviron-

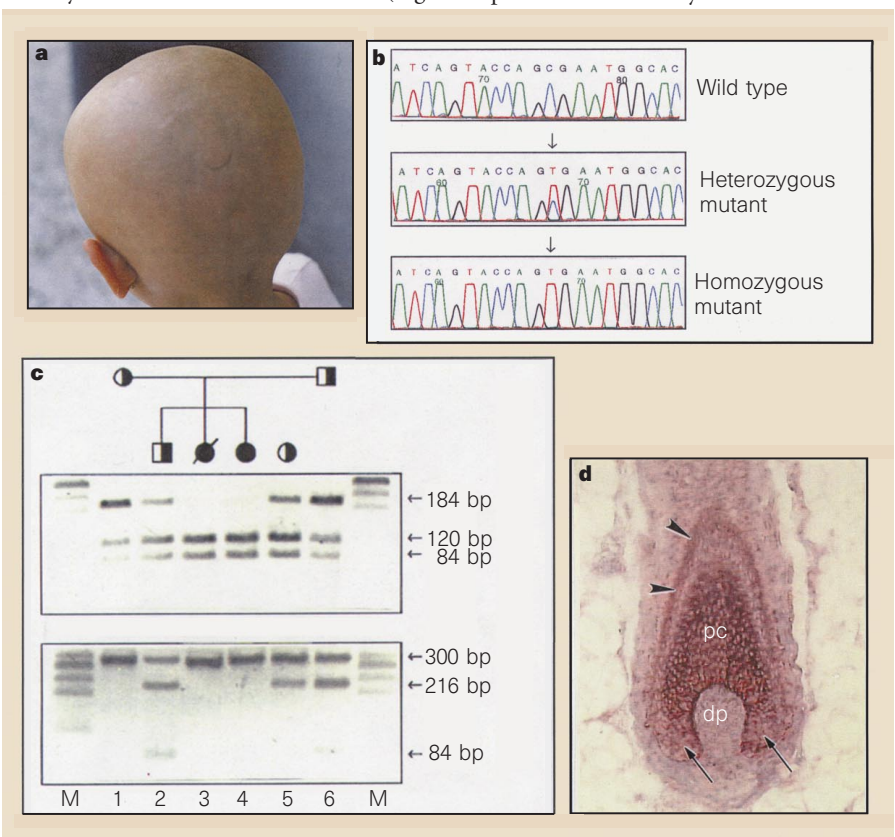

Figure 1 Molecular analysis of the human *nude* phenotype. **a,** A five-year-old child with congenital alopecia and T-cell immunodeficiency. **b,** Sequence analysis of a nonsense mutation in exon 5 of the *WHN* gene. Top, homozygous wild-type sequence from an unrelated, unaffected control individual. Middle, sequence from a heterozygous carrier of the mutation R255X; arrow indicates a double T+C peak. Bottom, homozygous mutant R255X sequence from the affected individual; arrow indicates mutant T only, leading to a C-to-T transition (CGA to TGA) and a substitution of an arginine residue by a nonsense mutation. **c,** Restriction-enzyme digestion confirms the mutation. The mutation introduced a restriction site for *BsrI* and, after digestion of the 184-base-pair (bp) polymerase chain reaction (PCR) product containing exon 5, the product generated from the mutant allele should cleave into two bands of 120 and 64 bp. Top, the unaffected parents and brother had three bands of 184, 120 and 64 bp (lanes 1, 2 and 6), indicating that they were heterozygous carriers of the mutation R255X. Both patients had only the two digested bands of 120 and 64 bp (lanes 3 and 4), consistent with the presence of the mutation in the homozygous state. Bottom, evidence for long-term engraftment of the bone-marrow transplant. Gender determination of family members revealed a genotypically XX pattern of an undigested 300-bp band in the mother (lane 1) and affected patients (lanes 3 and 4), and a genotypically XY pattern consisting of the 300-bp band and two additional bands of 216 and 84 bp, indicative of the Y chromosome, in the brother (lane 2) and father (lane 6). Lane 5, peripheral blood leukocytes from the patient after the transplant, demonstrating an XY genotype and the presence of the normal *WHN* allele, providing evidence for fraternal chimaerism and persistence of the graft. M, size markers. **d,** *WHN* mRNA expression in normal human scalp skin. In the hair bulb, *WHN* mRNA is localized to the differentiating cells of the hair follicle precortex (pc) and the innermost cell layer of the outer root sheath (arrowheads); the dermal papilla (dp) fibroblasts and hair matrix below the level of Auber (small arrows) remain negative for *WHN* mRNA.

ment in determining the T-cell repertoire, as both positive and negative selection of developing T cells depends on cell–cell interactions with the thymic epithelium. In *whn*-knockout mice, the defect has been localized to the differentiating thymic microenvironment rather than to a defect in the developing T cells[7]. The proband was free of infections for four years after the bone-marrow transplant, indicating that T-cell function was at least partly restored. This is probably due to mature T cells of donor origin, although we cannot exclude the possibility that positive selection of T lymphocytes occurs in the periphery despite the mutated *whn* gene.

Our findings provide evidence of a human immunodeficiency caused by a gene expressed not in haematopoietic cells[10], but in specific epithelial cells. In the human hair follicle, expression of *WHN* is sharply demarcated in defined cell populations (Fig. 1d). Although *nude* mice appear to be completely naked, the dermis contains a normal number of hair follicles, but they are incompletely developed. The fact that only short, bent hairs occasionally emerge from the epidermis is thought to result from impaired keratinization[11]. Together with the *hairless* gene[1], our finding extends the evidence implicating cell-type-specific transcription factors in hair-follicle cycling and morphogenesis, and indicates that baldness is an extremely complex phenotype.

Jorge Frank*, Claudio Pignata†, Andrei A. Panteleyev*, David M. Prowse‡, Howard Baden‡, Lorin Weiner‡, Lucia Gaetaniello†, Wasim Ahmad*, Nicola Pozzi†, Peter B. Cserhalmi-Friedman*, Vincent M. Aita¶, Hendrik Uyttendaele*, Derek Gordon§, Jurg Ott§, Janice L. Brissette‡, Angela M. Christiano*¶

*Departments of *Dermatology and ¶Genetics and Development, Columbia University, New York, New York 10032, USA*
e-mail:amc65@columbia.edu
†Department of Pediatrics, Unit of Immunology, Federico II University, Naples, Italy
‡Cutaneous Biology Research Center, Massachusetts General Hospital, and Department of Dermatology, Harvard Medical School, Charlestown, Massachusetts 02129, USA
§Laboratory of Statistical Genetics, The Rockefeller University, New York, New York 10021, USA

1. Ahmad, W. *et al. Science* **279,** 720–724 (1998).
2. Flanagan, S. P. *Genet. Res.* **8,** 295–309 (1966).
3. Nehls, M., Pfeifer, D., Schorpp, M., Hedrich, H. & Boehm, T. *Nature* **372,** 103–107 (1994).
4. Pignata, C. *et al. Am. J. Med. Genet.* **65,** 167–170 (1996).
5. Schorpp, M., Hoffmann, M., Dear, T. N. & Boehm, T. *Immunogenetics* **46,** 509–515 (1997).
6. Kaufmann, E. & Knöchel, W. *Mech. Dev.* **57,** 3–20 (1996).
7. Nehls, M. *et al. Science* **272,** 886–889 (1996).
8. Brissette, J. L., Li, J., Kamimura, J., Lee, D. & Dotto, G. P. *Genes Dev.* **10,** 2212–2221 (1996).
9. Muller-Hermelink, H. K., Wilisch, A., Schultz, A. & Marx, A. *Arch. Histol. Cytol.* **60,** 9–28 (1997).
10. Fischer, A. *et al. Annu. Rev. Immunol.* **15,** 93–124 (1997).
11. Köpf-Maier, P. *et al. Acta Anat.* **139,** 178–190 (1990).

Putting nuclear-test monitoring to the test

On the 22 August 1998, 0.1 kilotonnes of conventional explosives was fired underground at the nuclear test site of the former Soviet Union at Degelen Mountain in eastern Kazakhstan. This explosion, which we refer to as K980822, was carried out by the Republic of Kazakhstan, in cooperation with the United States, to seal tunnels at the site. It provided an opportunity to assess the network of seismological stations being set up as part of the International Monitoring System (IMS) to verify the Comprehensive Test Ban by detecting and identifying low-magnitude disturbances. Despite its low yield, short-period signals from the explosion were recorded up to 88° away. The seismograms recorded are sufficient to identify the disturbance as suspicious and, if the test-ban treaty were in force, could have led to a demand for an on-site inspection to determine whether a nuclear test had taken place.

The prototype International Data Center at Arlington, Virginia, detected short-period P-wave signals from the explosion at ten stations (Fig. 1), and estimates of the epicentre are within 12 km of the true epicentre. (The International Data Centre proper, which will provide data from the IMS to allow signatories to verify the test ban, is being set up in Vienna.) A weak P signal was also detected at Alice Springs, Australia (Fig. 1). The body-wave magnitude (m_b) was estimated to be 3.8. There were no observations of long-period (about 20 s) surface waves from the explosion.

The absence of surface waves at Zalesovo in the Russian Federation, only 6° from the epicentre, does not suggest an earthquake. For an earthquake of m_b 3.8, the surface-wave magnitude (M_s) is on average around 3.5, whereas for underground explosions at Degelen Mountain, $m_b - M_s$ is usually greater than one magnitude unit. Failure to detect a surface wave at Zalesova implies that $M_s < 2.3$, so the disturbance seems explosion-like. But some earthquakes in eastern Kazakhstan are 'anomalous events' in that, on the $m_b - M_s$ criterion, they look like explosions[1,2], so this criterion alone is insufficient. These earthquakes are usually easily identified because clear reflections (echoes) from the free surface (pP and sP), which travel from source to reflection point as P and S waves, respectively, and then on to the recording station as P waves, are seen, implying source depths of around 20 km, deeper than the maximum at which an explosion could be buried[1,2].

Of the seven stations that detected P-waves at long range (distances of more than 30°), most show simple signals that are typical of explosions, with the amplitude in the first 2–3 s after onset being significantly larger than the coda. The seismograms from three seismometer arrays detecting the disturbance are shown in Fig. 2. To confirm the presence of the signals, each array is considered as two sub-arrays with roughly equal numbers of elements, and the summed seismograms from each sub-array (the semi-sums) are formed separately. The semi-sums filtered in a 1.5–3.0 Hz passband are then multiplied together point by point. The product for the three stations is positive, confirming the presence of coherent arrivals (Fig. 2).

If the seismograms had been from an earthquake deeper than a few kilometres, then surface reflections would be expected at some of the stations. But the radiation pattern of the double-couple source — the accepted model of an earthquake — is not uniform, so the absence of visible surface reflections may be due to the orientation of the double-couple resulting in weak surface reflections relative to *P*. This can be tested by searching for orientations of a double-couple source that are compatible with the relative amplitudes of *P*, *pP* and *sP* and their polarities, where these can be observed unambiguously[4,5]. In practice, the method involves placing bounds on the amplitudes of *P* and possible surface reflections to allow for uncertainties in the measurements (Fig. 2). No orientation of a double-couple is found that is consistent with these bounds.

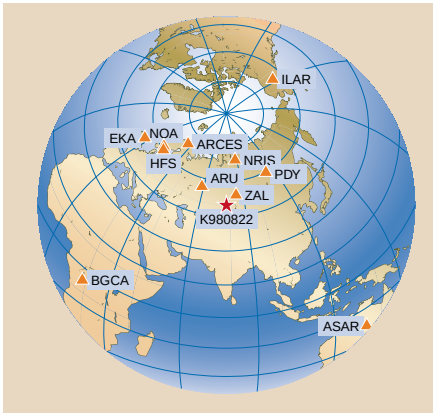

Figure 1 Azimuthal equal-area projection of the Earth, centred on the epicentre of K980822, showing the IMS stations that recorded seismic waves. Origin time, 05:00:18.94 UTC; estimated origin time, 05:00:18.7 UTC. Epicentre, 49.7667° N, 77.9908° E; estimated epicentre, 49.7566° N, 77.8273° E. Depth, 0.140 km. Firing medium, granite. Explosive, 100 tonnes of Granutoll. Estimates are from the prototype International Data Centre's *Reviewed Event Bulletin*. ARCES, Karasjok, Norway; ARU, Arti, Russian Federation; ASAR, Alice Springs, Australia; BGCA, Bangui, Central African Republic; EKA, Eskdalemuir, UK; HFS, Hagfors, Sweden; ILAR, Eielson, Alaska, USA; NOA, Hamar, Norway; NRIS, Norilsk, Russian Federation; PDY, Russian Federation; ZAL, Zalesovo, Russian Federation.